Chemical sensing with nanowires using electrical and optical detection

Matt Law, Donald J. Sirbuly and Peidong Yang*

Department of Chemistry,
University of California,
Berkeley, CA 94720, USA

Materials Sciences Division,
Lawrence Berkeley National Laboratory,
Berkeley, CA 94720, USA
Fax: 510 642 7301 E-mail: mlaw@berkeley.edu
E-mail: sirbuly2@llnl.gov E-mail: p_yang@berkeley.edu
*Corresponding author

Abstract: Chemical nanosensors based on inorganic nanowires hold promise for the extremely sensitive, direct detection of pollutants, toxins and biomolecules on platforms small enough to be integrated on optoelectronic chips or even deployed in living organisms. This paper discusses two approaches to nanowire-based chemical and biological detection. First we review the development of electrically-driven nanowire gas sensors that function by an adsorbate-mediated conductivity mechanism. We then describe an alternative sensing strategy that exploits the excellent waveguiding ability of high-refractive-index nanowires to create subwavelength evanescent wave sensors that operate in solution with an optical, rather than electrical, readout.

Keywords: nanowire; nanoribbon; tin dioxide; zinc oxide; chemical sensor; nanosensor; waveguide; subwavelength; evanescent field.

Reference to this paper should be made as follows: Law, M., Sirbuly, D.J. and Yang, P. (2007) 'Chemical sensing with nanowires using electrical and optical detection', *Int. J. Nanotechnol.*, Vol. 4, No. 3, pp.252–262.

Biographical notes: Matt Law received BA Degrees in Chemistry and Government (International Relations) from Wesleyan University in 1999 and is currently a graduate student in Materials Chemistry with Peidong Yang at the University of California, Berkeley, working on nanowire-based sensing, photonics and photovoltaics. He was named a 2005 Young Investigator by the Division of Inorganic Chemistry of the American Chemical Society. His research interests are energy conversion and storage, chemical sensing, pollution remediation and the conservation of biodiversity.

Donald J. Sirbuly received a BS Degree in Chemistry from Westmont College, Santa Barbara, CA in 1998 and PhD in Inorganic Chemistry from the University of California, Santa Barbara in 2003. Since 2003 he has been a Postdoctoral Researcher with Professor Peidong Yang at the University of California, Berkeley. At Berkeley he has worked on high dielectric subwavelength optical components and has interests in building functional spectroscopic and analytical devices with low-dimensional nanomaterials.

Peidong Yang received a BS in Chemistry from the University of Science and Technology of China in 1993 and a PhD in Chemistry from Harvard University in 1997. He did Postdoctoral research at University of California, Santa Barbara before joining the Faculty in the Department of Chemistry at the University of California, Berkeley in 1999. He is the recipient of Alfred P. Sloan research fellowship, the Arnold and Mabel Beckman Young Investigator Award, National Science Foundation Young Investigator Award, MRS Young Investigator Award, Julius Springer Prize for Applied Physics, and ACS Pure Chemistry Award. His main research interest is in the area of one dimensional semiconductor nanostructures and their applications in nanophotonics, energy conversion and nanofluidics. More about the Yang group research can be found in http://www.cchem.berkeley.edu/~pdygrp/main.html.

1 Introduction

Solid-state chemical sensors are an important class of devices for the detection of molecules in industry, medicine, environmental monitoring and homeland security. There is an increasingly critical need for small, cheap and reusable sensors that are capable of the rapid, sensitive, specific and multiplexed (i.e., parallel) identification of the components of chemical mixtures such as blood or urban air. Miniaturised sensors with real-time detection could be widely applied in high-throughput diagnostics for drug discovery and pre-symptomatic disease recognition.

Inorganic nanowires are especially suited to chemical sensing when configured as active channels for a flow of electrons or photons that can be modulated by molecules at the nanowire surface. When electrical current is monitored, molecules adsorbing onto a nanowire affect a change in conductivity by charge transfer and electrostatic gating, and the sensor is called a chemi-resistor. Most nanowire nanosensors use the chemi-resistor design because of its simplicity and potential for very high sensitivity. When a nanowire is configured to guide light rather than charge, nearby molecules can interact with its surrounding evanescent optical field by absorption or scattering, and the device is known as an evanescent wave sensor. Chemically synthesised, single-crystalline nanowires are ideal elements for both types of sensors because

- they are narrow diameter, high surface area conduits that maximise the influence of the surrounding chemical environment on the monitored signal
- their entire surface is readily accessible to analyte molecules, allowing for a rapid sensor response
- they are mechanically and chemically robust
- they can be functionalised with surface receptors for highly specific chemical detection, particularly in liquids
- they can be assembled into multi-wire architectures for the implementation of multiplexed sensing schemes.

We review here two nanowire-based approaches to chemical/biological sensing that detect the presence of analyte molecules at the nanowire surface. In the first example, single SnO_2 nanoribbons are configured as chemi-resistors to detect NO_2 at room

temperature. The second approach involves using single nanoribbons as evanescent wave sensors to detect nearby molecules in solution by fluorescence or absorbance mechanisms.

2 SnO_2 nanoribbon gas sensors

The conductivity of many metal oxides depends sensitively on the gases and vapours adsorbed on their surfaces from the surrounding environment. For *n*-type materials such as nominally undoped SnO_2, the adsorption of oxidising (reducing) species causes a decrease (increase) in surface electrical conductivity, principally by an electron trapping (donating) mechanism. The magnitude of the conductivity change is determined in general by the adsorption energy and in particular by the degree of adsorbate/oxide charge transfer. Chemical reactions between adsorbates also play a major part in dictating the conductivity response to certain molecules. For instance, combustible gases are known to scavenge adsorbed oxygen ions (O^-, O_2^- and O^{2-}) from the SnO_2 surface, thereby causing an increase in conductance far larger than what is expected from direct electron donation [1]. Metal oxide gas sensors usually operate at temperatures of 250–500°C to activate this surface chemistry and to make adsorption dynamic for real-time sensing.

It is possible to use optical rather than thermal means to activate a chemi-resistive gas sensor. The conductivity of semiconducting oxide nanowires is substantially enhanced when they are bathed in photons of energy greater than their bandgaps. Several years ago, we showed that the photoconductivity of ZnO nanowires could be exploited to create fast and reversible UV optical switches with ON-OFF switching ratios of four to six orders of magnitude under low-intensity 365 nm light [2]. The photocurrent in *n*-type oxide nanowires is a product of electron-hole pair formation and electron doping caused by the photo-induced desorption of oxidising surface species, including oxygen. We found that the strong photoresponse of individual SnO_2 nanoribbons makes it possible to achieve favourable adsorption-desorption kinetics for many gases at room temperature by illuminating the devices with ultraviolet (UV) light of energy near the SnO_2 bandgap ($E_g \approx 3.6$ eV at room temperature). We focus here on NO_2 because it is a combustion product with a key role in tropospheric ozone formation and a strongly binding electron-withdrawing adsorbate on SnO_2 surfaces [3]. Figure 1 illustrates the operational concept of a room-temperature nanoribbon gas sensor. During sensor operation, NO_2 adsorption traps free electrons and widens the region of depleted electron density near the ribbon surface, thereby causing its conductivity to drop, while the UV light continuously desorbs NO_2 to make the sensing dynamic. Thin nanoribbons (with diameters comparable to twice the depth of the surface depletion layer) essentially act as field-effect transistors with chemical gates that are continuously refreshed by photo-desorption.

We fabricated chemi-resistor gas sensors from individual SnO_2 nanoribbons dispersed across prefabricated gold electrodes on a silica surface. The synthesis of the nanoribbons is described elsewhere [3]. The single-crystalline nanoribbons have quasi-rectangular cross-sections bounded by the {101} and {010} rutile planes, with widths/thicknesses ranging from 30–300 nm and lengths of up to a millimetre. For testing, single-ribbon devices were wired to a chip carrier and mounted in a homemade gas flow cell equipped with multiple gas inlets, a quartz window for UV illumination and a turbomolecular

pump capable of 5×10^{-5} mbar operation. The UV source was a handheld lamp operated at either 254 nm or 365 nm with a power density at the sample of ~0.5 mW cm^{-2}.

Figure 1 The room-temperature nanoribbon NO_2 sensor. (a) The device geometry. (b) Cross-sectional view of a nanoribbon in NO_2 ambient in the dark and under UV illumination. Ambient NO_2 levels are tracked by monitoring changes in conductance in the illuminated state. Reproduced with permission. Copyright 2002 Wiley-VCH Verlag GmbH

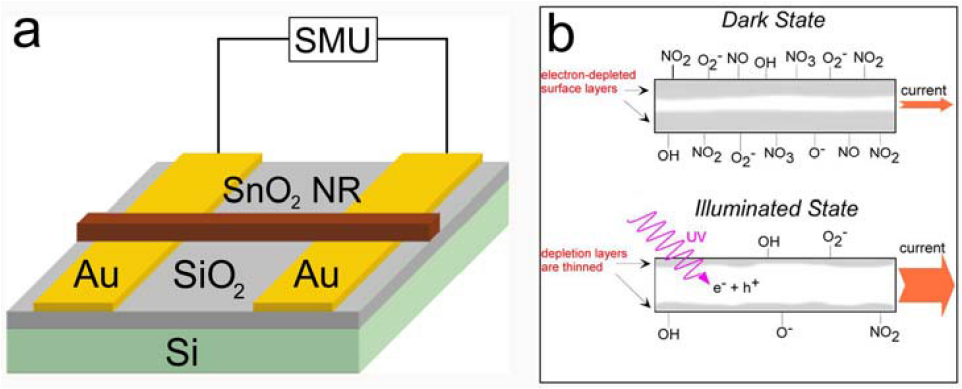

Figure 2(a) shows a typical time trace of nanoribbon photoresponse to alternating exposures of 254-nm light and 365-nm light in air and in 100 ppm NO_2. The conductance of the nanoribbon is larger in air than it is in the presence of NO_2 because of the greater oxidising ability of NO_2 relative to O_2. The conductance ratio for this particular ribbon is ~45 under 365-nm illumination, which suggests a minimum detectable NO_2 concentration of approximately 1–5 ppm. Figure 2(b) shows the photocurrent decay for a nanoribbon sensor in vacuum, air, and 100 ppm NO_2 environments after exposure to 254 nm illumination. Decay times get shorter and dark currents smaller in the sequence vacuum > air > 100 ppm NO_2, which reflects the availability of gas phase molecules for adsorption and the electron-trapping nature of NO_2.

The nanoribbon sensors are capable of rapidly and reversibly detecting NO_2 at concentrations as low as 2 ppm. A time trace of one sensor being cycled through various NO_2 concentrations is shown in Figure 3(a). The upward drift in baseline signal evident in this time trace was observed in a minority of devices and is most likely caused by unstable electrical contacts in our ribbon-on-electrode geometry. Figure 3(b) follows a second ribbon sensor as it was repeatedly cycled between air and 3 ppm NO_2. This behaviour was stable for more than 20 cycles without appreciable drift and with response times of less than a minute. These data show that single SnO_2 nanoribbons are small, fast and sensitive devices for detecting ppm-level NO_2 at room temperature under UV light.

Recently we carried out density functional theory (DFT) calculations to understand the details of molecular adsorption of O_2 and NO_2 on SnO_2 nanoribbon surfaces [4]. We found that

- oxygen chemisorbs only on surfaces that contain oxygen vacancies
- adsorbed NO_2 exists primarily as tightly bound NO_3 species, a finding that was confirmed with X-ray absorption near-edge spectroscopy (XANES)
- many surface species are mobile at room temperature and some can oxidise the SnO_2 lattice itself, potentially causing signal drift in nanowire NO_2 sensors.

Over the past few years, several studies by other groups have extended nanowire-based gas sensing to ZnO nanobelts, In_2O_3 wires, polycrystalline and Pd-decorated SnO_2 wires, and TiO_2 tubes arrays [5]. Particularly noteworthy is the demonstration by Zhou et al. of In_2O_3 nanowire field-effect transistors capable of detecting 5 ppb NO_2 at room temperature [6].

Figure 2 (a) Photoresponse of a single nanoribbon in pure air (triangles) and 100 ppm NO_2 (circles). The large peaks of both curves correspond to 254 nm UV illumination, the small peaks to 365 nm illumination, and the troughs to dark current. The air-to-NO_2 signal ratio is 45 : 1 under 365 nm light and 4 : 1 under 254 nm light. Note the shorter decay times in the presence of NO_2. Bias is 1.0 V. (b) Initial decay of the 254-nm photoresponse for a nanoribbon in vacuum (circles), air (triangles), and 100 ppm NO_2 (crosses). 99.9% decay in vacuum took over 4 h, while the signals in air and NO_2 decayed fully in about 300 and 200 s, respectively. Bias is 0.5 V. Reproduced with permission. Copyright 2002 Wiley-VCH Verlag GmbH

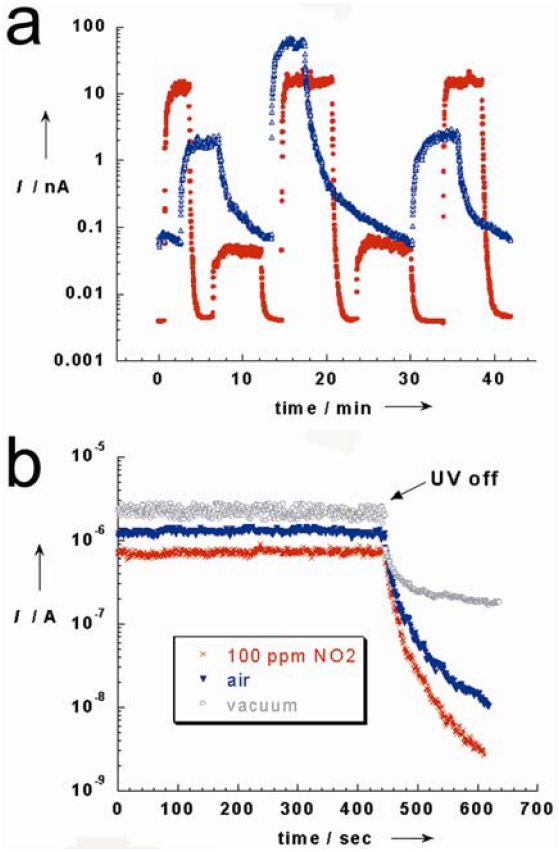

Figure 3 (a) Sensor response to different NO_2 concentrations when operated at 365 nm. The response time is 2–4 minutes. Vertical bars indicate periods when NO_2 flow was on. (b) Cycling a nanosensor near its resolution limit under 365 nm light. NO_2 concentrations are indicated. Horizontal bars are signal averages. Bias is 0.5 V. Reproduced with permission. Copyright 2002 Wiley-VCH Verlag GmbH

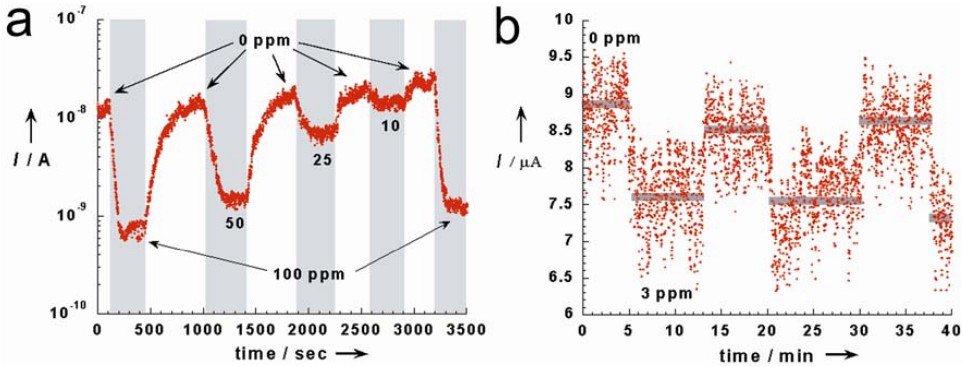

The high surface-to-volume ratio of thin nanowires endows them with inherently high sensitivity and short response times; however, selectivity is a major problem, especially in the detection of gases and gas mixtures. Despite decades of effort, a practical way to quantitatively identify the components of complex gas mixtures using oxide-based chemi-resistive sensors remains an elusive, and perhaps infeasible, goal. Selectivity is much more easily achieved in solution, where ligand-receptor binding and other surface functionalisation schemes can provide nearly perfect molecular discrimination. Lieber et al. have pioneered this approach for the detection of single macromolecules and viruses on functionalised silicon nanowires [7].

3 Nanoribbon evanescent wave sensors

Wide bandgap nanowires and nanoribbons are excellent subwavelength waveguides for UV and visible light. ZnO, GaN and CdS nanowire/nanoribbon lasers have been studied by several groups [8]. Recently we demonstrated that high aspect ratio SnO_2 nanoribbons with diameters below the wavelength of light (typically 100–400 nm) can guide both their own photoluminescence (PL) and the nonresonant UV/visible light emitted from adjacent, evanescently coupled nanowires, over distances of hundreds of microns [9]. Assemblies of nanowire light sources, waveguides, modulators and detectors may form the basis of a new class of optical circuitry for communications and computing. In addition, nanowire/ribbon waveguides are interesting structures for in vitro, and potentially in vivo, chemical and biological detection using light.

A subwavelength waveguide can carry a substantial fraction of its guided power outside of itself in the form of an evanescent wave that penetrates a short distance into the surroundings. In fibre-based evanescent wave sensing, the external field of a naked fibre is used to excite nearby molecules that can then be detected via absorption, fluorescence or scattering. The degree of optical confinement within a step-index fibre depends on several parameters, including the fibre radius (ρ) and cross-sectional shape, the wavelength of the guided light (λ) and the difference in the refractive index between

the fibre (n_{co}) and its surroundings (n_{cl}). For a cylindrical fibre, the fraction of the fundamental modal power carried within the core is given approximately by [10],

$$\eta = 1 - \frac{5.784 \exp -(2/V)}{V^3}$$

where $V = (2\pi\rho(n_{co}^2 - n_{cl}^2)^{1/2})/\lambda$. Smaller V thus results in more power carried outside of the core, where it is available to excite analyte species. For a given core/cladding combination, the use of a thinner waveguide or a longer wavelength puts proportionally more power into the evanescent wave. Figure 4 shows the fractional power in the core as a function of wavelength for cylindrical SnO_2 waveguides ($n \approx 2.1$ at 500 nm) in water ($n \approx 1.33$). Reducing V also increases the penetration depth of the field into the surrounding solution. The penetration depth increases quasi-exponentially as V decreases to small values, while the volume of solution probed by the evanescent wave passes through a weak minimum before it grows large for very thin waveguides (Figure 5). The evanescent field of a SnO_2 waveguide immersed in water and routing 500-nm light decays to 10% of its intensity at the centre of the waveguide approximately 130 nm, 137 nm, 159 nm and 310 nm into the solution for waveguides with diameters of 400 nm, 300 nm, 200 nm and 100 nm, respectively (see Figure 5). This corresponds to a probe volume of 2–4 fL for a path length of 10 μm and represents 1200–2400 analyte molecules for a 1 μM solution. In principle, therefore, nanowire waveguides are capable of detecting small numbers of molecules in sub-femtoliter volumes and with a large dynamic range.

Figure 4 Calculated fractional core-contained power vs. wavelength for SnO_2 waveguides of several diameters ($d = 2\rho$) in water

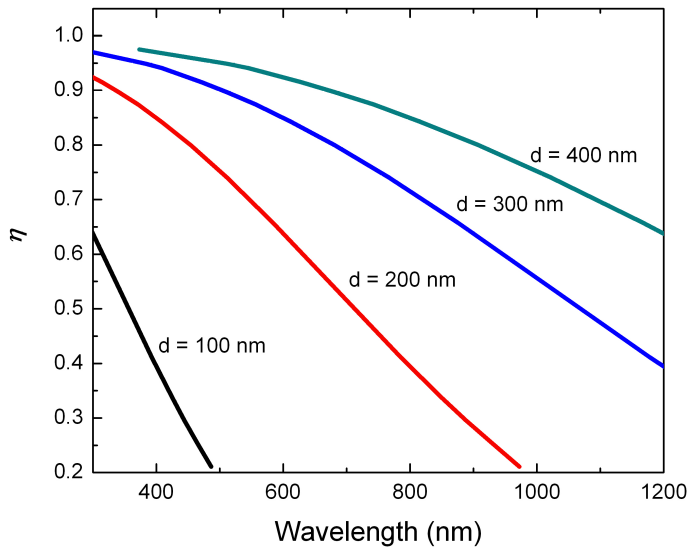

Figure 5 (a) Calculated penetration depth vs. V at different wavelengths for SnO_2 waveguides in water. Waveguide diameter vs. V is also plotted (right axis). (b) Probe volume against waveguide diameter at different wavelengths, assuming a path length of 10 μm. The calculation is made for $1 < V < 4$. Note that the waveguide diameter needed to minimise the probe volume varies from 150 nm for $\lambda = 400$ nm to 260 nm for $\lambda = 600$ nm

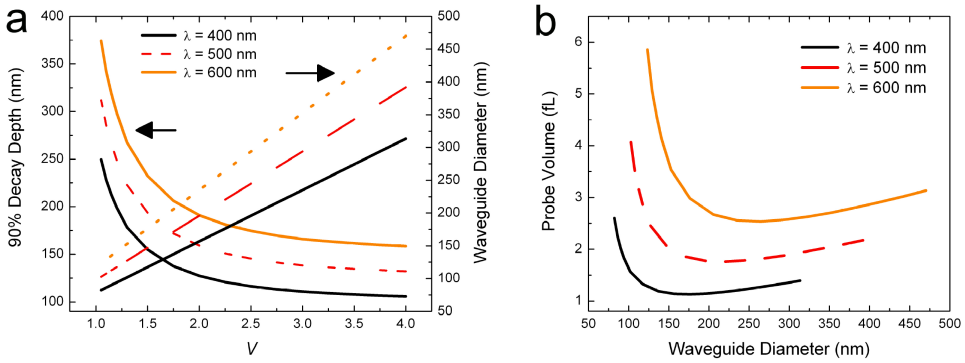

The attenuation of light in a fibre waveguide with absorbing molecules within its evanescent field follows a modified form of Beer's law. If scattering in the solution is negligible, the extinction of the guided intensity at a given wavelength is:

$$-\log\left(\frac{I}{I_0}\right) = \alpha c L f + \log\left(\frac{NA_0^2}{NA^2}\right)$$

where α is the absorption coefficient of the analyte solution, c is the analyte concentration, L is the path length, f is the fractional power carried in the evanescent field and $NA = (n_{co}^2 - n_{cl}^2)^{1/2}$. Here, the first term describes direct absorption of the waveguided light, while the second term provides a small correction to account for changes in the refractive index of the solution caused by the presence of the analyte.

We first show that SnO_2 nanoribbons can be used to produce an absorption spectrum of the surrounding solution. To demonstrate such an absorbance scheme, we launched white PL down a long ribbon resting on a silica surface onto the midpoint of which a 1 pL droplet of 1,5-pentanediol containing 1 mM rhodamine 6G (R6G, $\alpha_{max} = 535$ nm) was deposited (Figure 6). The dye in the droplet imprinted its absorption profile onto the guided PL transmitted to the opposite end of the ribbon. Considering the dye concentration, droplet size, and penetration depth of the evanescent field, we estimate that <40 attomoles of dye (~25 million molecules) were probed in this experiment. R6G concentrations down to 1 μM could be detected without optimisation; furthermore, by using a pure solvent droplet as a background, the normal UV-Vis absorption spectrum of RG6 could be accurately reproduced (Figure 6(c)). Figure 6(d) shows similar absorbance data for eosin-5-isothiocyanate in water.

Figure 6 Nanoribbon-based evanescent wave sensing using absorbance. (a) The geometry for the absorbance experiments. The nanoribbon (240 × 260 × 540 μm) is pumped by the 325-nm line of a HeCd laser, and the PL that passes through the droplet of 1,5-pentanediol containing 1 mM R6G is collected at the far end of the ribbon. (b) Spectra of the transmitted light. The R6G completely quenches transmission around its absorption maximum, which is indicated by the arrow. (c) Measured absorbance spectra of 3.5 μM R6G in water (pH = 7). The path length is 50 μm. A normalised UV-Vis spectrum is included for comparison and offset for clarity. The baseline spectrum corresponds to pure solvent. (d) Absorbance spectra of 1 mM eosin-5-isothiocyanate in water (pH = 12), along with a normalised UV-Vis spectrum. Reproduced with permission. Copyright AAAS, USA

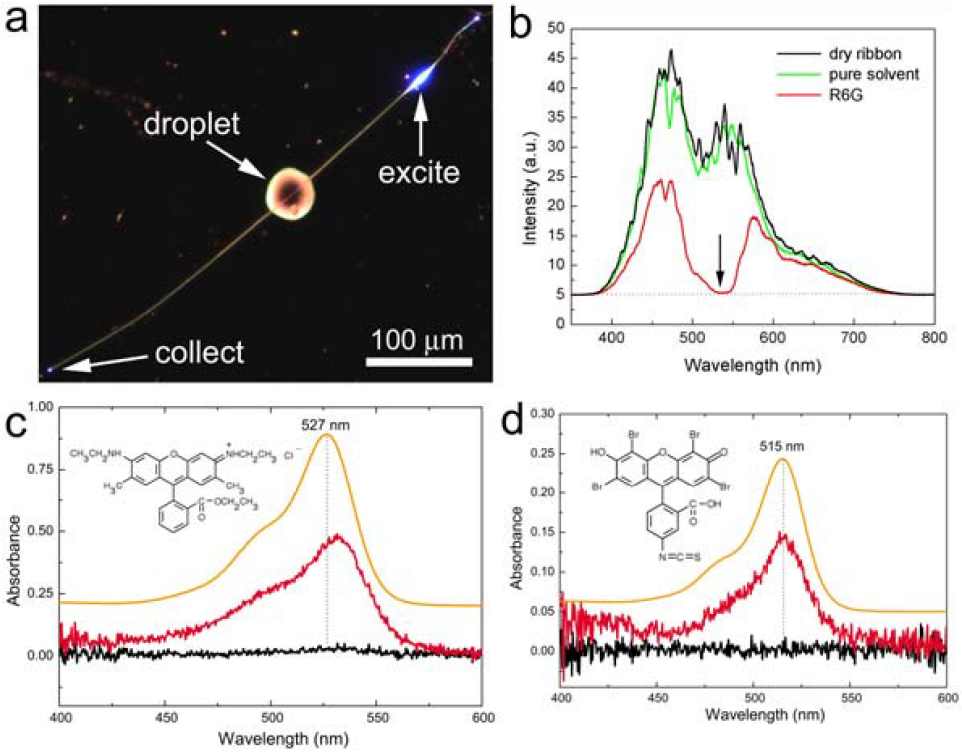

Fluorescence sensing can be accomplished by guiding monochromatic light through a nanoribbon waveguide that is in contact with a fluorophore-containing droplet. In Figure 7, blue light (442 nm) launched into the far end of a ribbon results in strong fluorescence from within a RG6-loaded droplet (1 mM), where the R6G emission maps out the spatial intensity distribution of the waveguide output as a cone of light. A fraction of this fluorescence is captured by the ribbon cavity and guided back to its far end, demonstrating that these waveguides are capable of routing signals both to and from liquids. The image in Figure 7(a) also shows strong fluorescence originating from the segment of the ribbon wet by the droplet through capillary action. Here, dye is pumped by the evanescent field that extends roughly 125 nm into the surrounding solution.

These simple demonstrations of evanescent wave sensing highlight the potential of miniaturised spectroscopic devices based on subwavelength optical elements, but leave much room for improvement. First, nanowire waveguides should be integrated with

microfluidics to achieve the rapid and controlled delivery of analyte species in a reusable device. Multiplexed sensing is possible with multi-wire, multi-channel microfluidic arrays. Multiplexed optical detection can be made more powerful by functionalising the nanowires/ribbons with surface receptors for the selective binding of macromolecules, viruses and other entities of diagnostic interest. Also, by properly decorating the nanowire surface with noble metal nanoparticles, our optical detection scheme can be extended to surface enhanced Raman scattering (SERS) to provide spectral fingerprints of molecules bound to the waveguide sensors. Finally, it may be advantageous to leverage the ability of semiconductor nanowires to guide both electrons and photons in order to combine electrical and optical detection for more advanced nanowire-based sensing systems.

Figure 7 Fluorescence sensing with single nanoribbon waveguides. (a) Fluorescence image of a droplet of 1 mM R6G in 1,5-pentanediol excited by blue light from a ribbon waveguide (the same ribbon used in Figure 4). The nanoribbon crosses the frames from upper left to lower right. A notch filter was used to block the excitation light. Inset is a dark-field image showing the droplet and the bottom half of the ribbon, as well as a magnified view of the droplet emission showing the light cone and evanescent pumping of the dye along the ribbon length. (b) Spectra taken of the droplet region (direct) and the fluorescence coupled back into the ribbon (guided). The redshift of the guided emission is a microcavity effect. Reproduced with permission. Copyright AAAS, USA

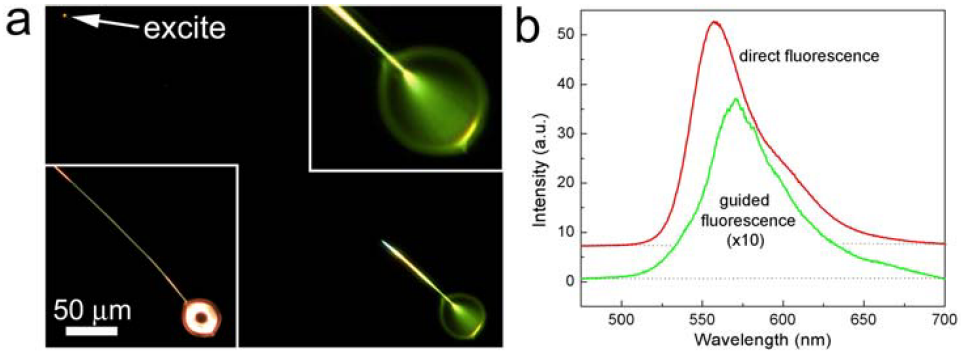

References

1 Watson, J., Ihokura, K. and Coles, G.S.V. (1993) 'The tin dioxide gas sensor', *Meas. Sci. Technol.*, Vol. 4, pp.711–719.

2 Kind, H., Yan, H., Messer, B., Law, M. and Yang, P. (2002) 'Nanowire ultraviolet photodetectors and optical switches', *Adv. Mater.*, Vol. 14, pp.158–160.

3 Law, M., Kind, H., Messer, B., Kim, F. and Yang, P. (2002) 'Photochemical sensing of NO_2 with SnO_2 nanoribbon nanosensors at room temperature', *Angew. Chem. Int. Ed.*, Vol. 41, pp.2405–2408.

4 Maiti, A., Rodriguez, J.A., Law, M., Kung, P., McKinney, J.R. and Yang, P. (2003) 'SnO_2 nanoribbons as NO_2 sensors: insights from first principles calculations', *Nano Lett.*, Vol. 3, pp.1025–1028.

5 (a) Comini, E., Faglia, G., Sberveglieri, G., Pan, Z. and Wang, Z.L. (2002) 'Stable and highly sensitive gas sensors based on semiconducting oxide nanobelts', *Appl. Phys. Lett*., Vol. 81, pp.1869–1871. (b) Kolmakov, A., Zhang, Y., Cheng, G. and Moskovits, M. (2003) 'Detection of CO and O_2 using tin oxide nanowire sensors', *Adv. Mater*., Vol. 15, pp.997–1000. (c) Varghese, O.K., Gong, D., Paulose, M., Ong, K.G., Dickey, E.C. and Grimes, C.A. (2003) 'Extreme changes in the electrical resistance of titania nanotubes with hydrogen exposure', *Adv. Mater*., Vol. 15, pp.624–627. (d) Kolmakov, A., Klenov, D.O., Lilach, Y., Stemmer, S. and Moskovits, M. (2005) 'Enhanced gas sensing by individual SnO_2 nanowires and nanobelts functionalized with Pd catalyst particles', *Nano Lett*., Vol. 5, pp.667–673.

6 Zhang, D., Liu, Z., Li, C., Tang, T., Liu, X., Han, S., Lei, B. and Zhou, C. (2004) 'Detection of NO_2 down to ppb levels using individual and multiple In_2O_3 nanowire devices', *Nano Lett*., Vol. 4, pp.1919–1924.

7 (a) Patolsky, F., Zheng, G., Hayden, O., Lakadamyali, M., Zhuang, X. and Lieber, C.M. (2004) 'Electrical detection of single viruses', *Proc. Natl. Acad. Sci. U.S.A.*, Vol. 101, pp.14017–14022. (b) Wang, W.U., Chen, C., Lin, K., Fang, Y. and Lieber, C. M. (2005) 'Label-free detection of small-molecule–protein interactions by using nanowire nanosensors', *Proc. Natl. Acad. Sci. U.S.A.*, Vol. 102, pp.3208–3212.

8 Huang, H.M., Mao, S., Feick, H., Yan, H., Wu, Y., Kind, H., Weber, E., Russo, R. and Yang, P. (2001) 'Room-temperature ultraviolet nanowire nanolasers', *Science*, Vol. 292, pp.1897–1899. (b) Johnson, J.C., Choi, H.J., Knutsen, K.P., Shaller, R.D., Yang, P. and Saykally, R.J. (2002) 'Single gallium nitride nanowire lasers', *Nat. Mater*., Vol. 1, pp.106–110. (c) Duan, X.F., Huang, Y., Agarwal, R. and Lieber, C.M. (2003) 'Single-nanowire electrically driven lasers', *Nature*, Vol. 421, pp.241–245. (d) Sirbuly, D.J., Law, M., Yan, H. and Yang, P. (2005) 'Semiconductor nanowires for subwavelength photonics integration', *J. Phys. Chem. B*, Vol. 109, pp.15190–15213.

9 Law, M., Sirbuly, D.J., Johnson, J.C., Goldberger, J., Saykally, R.J. and Yang, P. (2004) 'Nanoribbon waveguides for subwavelength photonics integration', *Science*, Vol. 305, pp.1269–1273. (b) Sirbuly, D.J., Law, M., Pauzauskie, P., Yan, H., Maslov, A.V., Knutsen, K., Ning, C.Z., Saykally, R.J. and Yang, P. (2005) 'Optical routing and sensing with nanowire assemblies', *Proc. Natl. Acad. Sci. U.S.A.*, Vol. 102, pp.7800–7805.

10 Snyder, A.W. and Love, J.D. (1983) *Optical Waveguide Theory*, Chapman and Hall, London.